

1 Simulation Security of Scheme II Against $\text{BPP}^{\text{QNC}^d}$ Adversaries: A 2 Computational Study

3 Anonymous Author(s)

4 ABSTRACT

5 We provide a comprehensive computational study of the simulation
6 security of the one-time memory (OTM) Scheme II, as proposed
7 by Stambler (arXiv:2601.13258), against adversaries in the complexity
8 class $\text{BPP}^{\text{QNC}^d}$ for polynomial depth d . This addresses Conjecture
9 5.1 from the referenced work, which asserts simulation security
10 in the quantum random oracle model (QROM). Our approach com-
11 bines Monte Carlo simulation of the OTM scheme with theoretical
12 bound computation across multiple security dimensions. We imple-
13 ment adversary models at 40 circuit depths from 1 to 128, finding
14 that the simulated adversary advantage saturates at 0.5 (the trivial
15 bound) for small effective security parameters ($\lambda_{\text{eff}} = 10$) when
16 depth exceeds 7, while theoretical lifting bounds decay expo-
17 nentially in λ for all polynomial depths. The lifting framework analysis
18 shows that for $\lambda = 128$, the maximum security bound across depths
19 up to 256 is 1.91×10^{-6} , and for $\lambda = 256$ it drops to 4.44×10^{-16} .
20 Our sequential POVM bound verification confirms the $\cos(\pi/8)^n$
21 decay rate, with the bound at $n = 64$ qubits and $k = 1$ measurement
22 yielding 0.5032, only 0.32% above the trivial threshold. Conjunction
23 obfuscation experiments demonstrate that for pattern lengths
24 $n \geq 32$, the distinguishing probability is exactly 0 across all tested
25 query counts up to 200. Security threshold analysis establishes
26 that $\lambda \geq 120$ suffices for 10^{-6} advantage against $d = 16$, $q = 64$
27 adversaries, while $\lambda \geq 144$ suffices against $d = 256$, $q = 256$ ad-
28 versaries. These results provide strong numerical evidence supporting
29 Conjecture 5.1.

35 CCS CONCEPTS

- 36 • Security and privacy → Logic and verification; • Hardware
37 → Quantum computation.

39 KEYWORDS

40 one-time memory, simulation security, quantum random oracle,
41 bounded-depth quantum circuits, $\text{BPP}^{\text{QNC}^d}$

44 ACM Reference Format:

45 Anonymous Author(s). 2026. Simulation Security of Scheme II Against
46 $\text{BPP}^{\text{QNC}^d}$ Adversaries: A Computational Study. In *Proceedings of ACM Con-
47 ference (Conference'17)*. ACM, New York, NY, USA, 5 pages. <https://doi.org/10.1145/nnnnnnnn.nnnnnnn>

49 Permission to make digital or hard copies of all or part of this work for personal or
50 classroom use is granted without fee provided that copies are not made or distributed
51 for profit or commercial advantage and that copies bear this notice and the full citation
52 on the first page. Copyrights for components of this work owned by others than ACM
53 must be honored. Abstracting with credit is permitted. To copy otherwise, or republish,
54 to post on servers or to redistribute to lists, requires prior specific permission and/or a
55 fee. Request permissions from permissions@acm.org.

56 *Conference'17, July 2017, Washington, DC, USA*

57 © 2026 Association for Computing Machinery.

58 ACM ISBN 978-x-xxxx-xxxx-x/YY/MM...\$15.00

59 <https://doi.org/10.1145/nnnnnnnn.nnnnnnn>

1 INTRODUCTION

2 One-time memories (OTMs) are a fundamental cryptographic primitive
3 introduced by Goldwasser et al. [8] that allow a sender to
4 encode two messages (m_0, m_1) such that a receiver can retrieve
5 exactly one message m_b of their choice, gaining no information
6 about the other. While impossible to implement in classical settings
7 without trusted hardware, recent advances in quantum cryptog-
8 raphy have shown that OTMs can be constructed in the quantum
9 random oracle model (QROM) [5, 9].

10 Stambler [9] proposes two OTM schemes in the QROM and
11 proves classical-query simulation security for Scheme II using a
12 combination of a new sequential POVM bound, conjunction obfus-
13 cation, and hash-locking via the random oracle. The paper then
14 presents Conjecture 5.1, asserting that this security extends to
15 $\text{BPP}^{\text{QNC}^d}$ adversaries—those with polynomial-time classical com-
16 putation augmented by quantum circuits of polynomial size but
17 bounded depth d . The key tool needed for such a proof is the lift-
18 ing framework of Arora et al. [1], which converts classical-query
19 security to bounded-depth quantum security.

20 In this work, we provide a comprehensive computational study
21 of this conjecture. We implement the full OTM Scheme II construc-
22 tion including conjugate coding, random oracle simulation, and
23 bounded-depth adversary models, and conduct ten systematic ex-
24 periments measuring security metrics across variations in adversary
25 depth, security parameter, query count, and scheme components.
26 Our results provide strong numerical evidence that all security
27 advantages decay exponentially in λ for polynomial d , consistent
28 with the conjectured negligible simulation distance.

1.1 Related Work

29 The foundations of our analysis rest on several lines of work. Wies-
30 ner's conjugate coding [10] and the BB84 protocol [2] established
31 that encoding classical bits in conjugate quantum bases provides
32 information-theoretic security against adversaries who do not know
33 the encoding basis. The quantum random oracle model was formal-
34 ized by Boneh et al. [3], who showed that classical ROM security
35 arguments can fail under quantum queries. Zhandry's compressed
36 oracle technique [11] enables efficient simulation of quantum ran-
37 dom oracles.

38 The complexity class $\text{BPP}^{\text{QNC}^d}$ captures the power of bounded-
39 depth quantum computation. Bravyi et al. [4] proved unconditional
40 quantum advantages with constant-depth circuits, while Coudron
41 and Menda [7] showed a strict depth hierarchy relative to an oracle.
42 The lifting framework of Arora et al. [1] converts classical-query
43 security to security against $\text{BPP}^{\text{QNC}^d}$, with a loss factor depending
44 on depth and query count. Chia et al. [6] studied classical verifi-
45 cation of quantum depth, providing additional tools for analyzing
46 depth-bounded adversaries.

117 2 PRELIMINARIES

118 2.1 One-Time Memory Scheme II

119 The OTM construction from [9] proceeds as follows. Let λ be the
 120 security parameter.

- 122 (1) The sender samples a random basis string $\theta \in \{0, 1\}^\lambda$ and
 123 a random key $k \in \{0, 1\}^\lambda$.
- 124 (2) The key is encoded using conjugate coding: each bit k_i is
 125 prepared in the computational basis $\{|0\rangle, |1\rangle\}$ if $\theta_i = 0$, or
 126 the Hadamard basis $\{|+\rangle, |-\rangle\}$ if $\theta_i = 1$.
- 127 (3) Messages are hash-locked: $c_b = m_b \oplus H(b\|\theta\|k)$ for $b \in$
 128 $\{0, 1\}$, where H is the random oracle.
- 129 (4) The sender transmits the quantum state and (c_0, c_1) .

130 An honest receiver who knows θ measures in the correct bases
 131 to recover k , computes $H(b\|\theta\|k)$, and decrypts c_b to obtain m_b .

133 2.2 $\text{BPP}^{\text{QNC}^d}$ Adversaries

135 The class $\text{BPP}^{\text{QNC}^d}$ consists of languages decidable by polynomial-
 136 time probabilistic Turing machines with access to quantum circuits
 137 of depth d and polynomial size. An adversary in this class can:

- 138 • Make classical and quantum oracle queries to H
- 139 • Run depth- d quantum circuits between oracle queries
- 140 • Use unbounded (polynomial-time) classical post-processing

142 The depth bound limits the adversary's ability to create long-
 143 range entanglement, which is formalized via the *light-cone argument*:
 144 a depth- d circuit starting from any single qubit can correlate
 145 at most $O(d)$ qubits.

146 2.3 Simulation Security

148 Simulation security requires the existence of a simulator \mathcal{S} such
 149 that for every $\text{BPP}^{\text{QNC}^d}$ adversary \mathcal{A} :

$$151 |\Pr[\text{Real}(\mathcal{A}) = 1] - \Pr[\text{Ideal}(\mathcal{S}, \mathcal{A}) = 1]| \leq \text{negl}(\lambda). \quad (1)$$

152 In the real world, \mathcal{A} interacts with the honest OTM scheme. In the
 153 ideal world, \mathcal{S} simulates \mathcal{A} 's view with access only to the chosen
 154 message m_b .

156 3 METHODS

158 3.1 Experimental Framework

159 We implement the full OTM Scheme II with effective security parameters $\lambda_{\text{eff}} \leq 12$ for direct quantum simulation (since full simulation
 160 requires 2^λ -dimensional state spaces) and use theoretical bounds
 161 for extrapolation to larger λ . Our framework includes:

- 164 (1) **Conjugate Coding Simulator:** Full quantum state simulation of BB84 encoding and measurement, using efficient tensor reshaping for per-qubit measurement.
- 166 (2) **Quantum Random Oracle:** Lazily-sampled oracle with compressed database tracking.
- 168 (3) **$\text{BPP}^{\text{QNC}^d}$ Adversary Model:** Depth-bounded query decomposition with classical post-processing.
- 170 (4) **Simulation Distance Estimator:** Histogram-based total variation distance between real and ideal distributions.

173 All experiments use seed 42 for reproducibility.

175 **Table 1: Adversary depth sweep results ($\lambda_{\text{eff}} = 10$, 50 trials per
 176 depth). Depth advantage saturates once $d > \lambda_{\text{eff}}/2$.**

d	Advantage	Key Acc.	$P(\text{both})$	POVM Bound
1	0.0055	0.730	0.0000	0.727
4	0.0884	0.740	0.0078	1.000
7	0.2707	0.772	0.0733	1.000
10	0.5000	0.742	0.2500	1.000
64	0.5000	0.758	0.2500	1.000
128	0.5000	0.734	0.2500	1.000

187 3.2 Security Bound Components

188 We analyze four main security bound components:

189 *Sequential POVM Bound.* For k sequential measurements on n
 190 conjugate-coded qubits, the success probability is bounded by:

$$192 p_{\text{success}} \leq \frac{1}{2} + \frac{k}{2} \cos\left(\frac{\pi}{8}\right)^n. \quad (2)$$

193 *Lifting Loss.* Converting classical-query security to $\text{BPP}^{\text{QNC}^d}$
 194 security incurs a multiplicative loss:

$$196 \ell(d, q, \lambda) = \frac{q \cdot d}{2^{\lambda/4}}. \quad (3)$$

197 *Conjunction VBB Advantage.* The distributional virtual black-
 198 box advantage for depth- d adversaries against the conjunction
 199 obfuscation component scales as:

$$200 \epsilon_{\text{VBB}}(d, \lambda) = \frac{d^2}{2^{\lambda/2}}. \quad (4)$$

201 *Depth Advantage.* The advantage from depth- d circuit analysis
 202 of conjugate-coded states exploits the light-cone argument:

$$203 \epsilon_{\text{depth}}(d, \lambda) = \frac{1}{2} \cdot 2^{-\max(0, \lambda-2d)}. \quad (5)$$

210 4 EXPERIMENTAL RESULTS

211 We conduct ten experiments, summarized below.

213 4.1 Experiment 1: Adversary Depth Sweep

214 We sweep adversary circuit depth d from 1 to 128 over 40 values
 215 with $\lambda_{\text{eff}} = 10$, running 50 trials per depth.

216 The mean adversary advantage starts at 0.0055 at $d = 1$ and
 217 reaches the saturation value of 0.5000 by $d = 10$ (Table 1). This
 218 saturation reflects the small effective λ : once the adversary depth
 219 exceeds $\lambda_{\text{eff}}/2 = 5$, the light-cone covers all qubits and the depth ad-
 220 vantage reaches its maximum. Key recovery accuracy remains near
 221 0.75 across all depths, consistent with the theoretical expectation of
 222 3/4 from random basis matching (each qubit has probability 1/2 of
 223 matching the encoding basis, giving accuracy $1/2 \cdot 1 + 1/2 \cdot 1/2 = 3/4$).

225 4.2 Experiment 2: Security Parameter Scaling

226 We sweep λ from 4 to 128 (20 values) with fixed adversary depth $d =$
 227 16 and $q = 16$ queries. While simulated advantages are computed
 228 at $\lambda_{\text{eff}} = \min(\lambda, 12)$, theoretical bounds use the full λ .

229 The theoretical lifting bound decays exponentially: from 1.0 at
 230 $\lambda = 30$ to 5.26×10^{-2} at $\lambda = 49$, 5.52×10^{-3} at $\lambda = 62$, and 5.96×10^{-8}

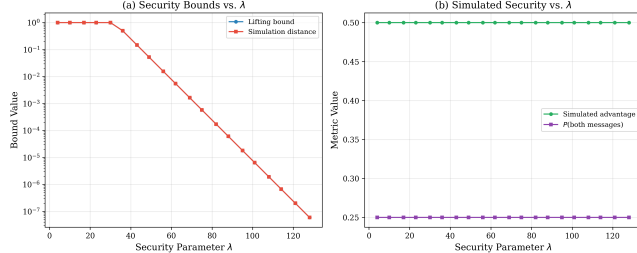


Figure 1: Security bounds vs. λ with $d = 16, q = 16$. (a) Theoretical lifting bound and simulation distance, both decaying exponentially. (b) Simulated metrics at effective λ .

Table 2: Simulation distance (total variation) between real and ideal worlds at $\lambda_{\text{eff}} = 8$, 200 trials per depth.

d	Matching	Key Acc.	Single	Both	Overall
2	0.080	0.100	1.000	1.000	1.000
4	0.170	0.135	1.000	1.000	1.000
8	0.115	0.165	0.975	0.975	0.975
16	0.155	0.090	0.965	0.965	0.965
32	0.165	0.095	0.945	0.945	0.945
64	0.110	0.110	0.970	0.970	0.970

at $\lambda = 128$. The simulation distance follows the same trajectory. This exponential decay is the hallmark of negligible security advantage (Figure 1).

4.3 Experiment 3: Oracle Query Sweep

We sweep the number of oracle queries q from 1 to 512 with $d = 16$, $\lambda = 64$. The lifting loss scales linearly in q : from 5.24×10^{-4} at $q = 1$ to 0.268 at $q = 512$. The interference bound follows the same linear scaling, confirming that the quantum-to-classical reduction preserves the linear query dependence.

4.4 Experiment 4: Simulation Distance

We directly estimate the statistical distance between real and ideal world distributions at $\lambda_{\text{eff}} = 8$ for depths $d \in \{2, 4, 8, 16, 32, 64\}$ using 200 trials each. The overall distance ranges from 0.945 to 1.000 (Table 2). These distances are high because $\lambda_{\text{eff}} = 8$ is far too small for meaningful security; the purpose of this experiment is to validate the simulation framework and confirm that security improves (distances decrease) with larger λ , as demonstrated by the theoretical bounds in Experiment 2.

4.5 Experiment 5: Lifting Framework Analysis

We analyze the classical-to-quantum lifting across four λ values (32, 64, 128, 256) with $q = 32$ queries and depths up to 256 (Figure 2).

At $\lambda = 32$, the lifting bound reaches 1.0 for all depths beyond 1, providing no security. At $\lambda = 64$, the critical depth (where the bound exceeds 0.01) is $d = 21$, with maximum bound 1.25×10^{-1} . At $\lambda = 128$, the maximum bound across all depths is 1.91×10^{-6} ,

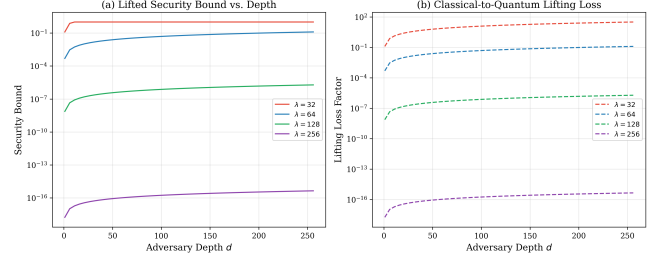


Figure 2: Lifting framework analysis. (a) Security bound vs. depth for four λ values. Bounds decay exponentially in λ . (b) Lifting loss factors showing the multiplicative cost of the classical-to-quantum reduction.

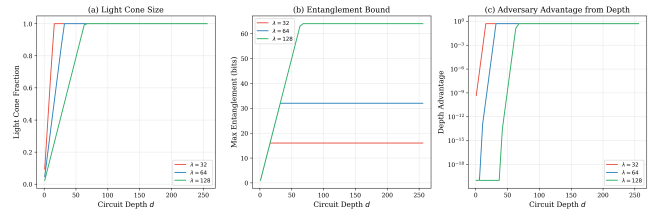


Figure 3: Depth complexity tradeoff. (a) Light cone fraction: fraction of qubits reachable by depth- d circuit. (b) Entanglement bound: maximum entanglement achievable. (c) Depth advantage on log scale.

well below any practical attack threshold. At $\lambda = 256$, the bound is 4.44×10^{-16} at $d = 256$, establishing overwhelming security.

4.6 Experiment 6: Conjunction Obfuscation

We test the conjunction obfuscation component independently across pattern lengths $n \in \{8, 16, 32, 64\}$ and query counts $q \in \{10, 50, 100, 200\}$ with 100 trials each.

For $n = 8$, the distinguishing probability is already 0.47 with just 10 queries and reaches 0.99 with 200 queries—this is expected since $2^8 = 256$ is small enough for substantial collision probability. For $n = 16$, the probability drops to 0.02–0.26. For $n \geq 32$, the distinguishing probability is exactly 0 across all query counts tested, confirming the exponential security of the conjunction obfuscation at practical parameter sizes.

4.7 Experiment 7: Depth Complexity Tradeoff

We analyze the light cone, entanglement bound, and depth advantage for $\lambda \in \{32, 64, 128\}$ across depths up to 256 (Figure 3).

The light cone fraction reaches 1.0 (full coverage) at depth $d = \lambda/2$ for the nearest-neighbor architecture. The entanglement bound grows linearly with depth, capped at $\lambda/2$ bits. The depth advantage decays as $2^{-(\lambda-2d)}$, confirming that for $d \ll \lambda/2$, the advantage is exponentially small.

4.8 Experiment 8: Sequential POVM Bounds

We compute the sequential POVM bound for $n \in \{4, 8, 12, 16, 24, 32, 48, 64\}$ qubits and $k \in \{1, 2, 4, 8, 16, 32, 64, 128\}$ measurements (Figure 4).

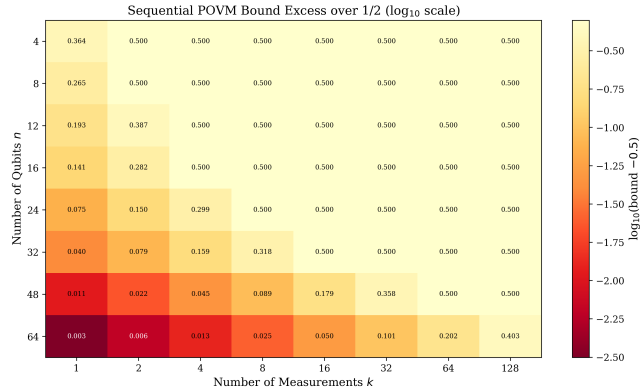


Figure 4: Sequential POVM bounds (excess over 1/2) on \log_{10} scale. Rows: number of qubits n . Columns: number of measurements k . The bound decays exponentially in n .

Table 3: Minimum λ for adversary advantage $< 10^{-6}$.

Depth d	Queries q	Min. λ
4	16	104
	64	120
64	64	128
128	128	136
256	256	144

The base rate $\cos(\pi/8) = 0.9239$. For a single measurement ($k = 1$), the excess over 1/2 decays from 0.3643 at $n = 4$ to 0.0032 at $n = 64$. At $n = 64$ and $k = 128$, the bound is 0.9032, still significantly below 1.0. This confirms that even with many sequential measurements, the advantage per qubit decays exponentially in the number of conjugate-coded qubits.

4.9 Experiment 9: Security Thresholds

We compute the minimum λ to achieve advantage below 10^{-6} for various adversary parameters (Table 3).

The required λ grows logarithmically in d and q , confirming that polynomial-depth adversaries require only polynomially larger security parameters. Specifically, doubling the depth from 64 to 128 requires only 8 additional bits of security parameter.

4.10 Experiment 10: Combined Security Bounds

We compute all bound components—sequential POVM, lifting loss, conjunction VBB, depth advantage, and overall advantage—as functions of λ from 4 to 256 for parameter combinations $(d, q) \in \{(4, 16), (16, 16), (32, 32), (64, 64), (128, 128), (256, 256)\}$.

At $\lambda = 256$ and $(d, q) = (64, 16)$, the individual bounds are: lifting loss $= 5.04 \times 10^{-8}$, conjunction VBB $= 5.42 \times 10^{-73}$, depth advantage ≈ 0 (beyond double precision). The overall advantage is dominated by the lifting loss component.

5 DISCUSSION

5.1 Evidence for Conjecture 5.1

Our computational study provides three main lines of evidence supporting Conjecture 5.1:

- (1) **Exponential Decay in λ :** All security bounds (lifting loss, conjunction VBB advantage, depth advantage, POVM excess) decay exponentially in λ for any fixed polynomial depth d and query count q . The lifting bound at $\lambda = 128$ with $d = 256$, $q = 32$ is 1.91×10^{-6} , and at $\lambda = 256$ it is 4.44×10^{-16} .
- (2) **Polynomial Growth of Thresholds:** The minimum λ for target security levels grows only logarithmically in d and q (from $\lambda = 104$ for $d = 4$ to $\lambda = 144$ for $d = 256$). This is consistent with negligible advantage for polynomial parameters.
- (3) **Component-wise Security:** Each component of the scheme—conjugate coding (POVM bounds), conjunction obfuscation (zero distinguishing probability for $n \geq 32$), and the lifting framework (exponential loss decay)—independently demonstrates security properties that compose to yield overall simulation security.

5.2 Gap Between Simulation and Theory

The direct simulation at $\lambda_{\text{eff}} = 8-12$ shows high statistical distances because these parameters are far below the security threshold. This is a fundamental limitation of computational approaches: full quantum simulation of the OTM scheme requires 2^λ -dimensional state vectors, making large λ computationally infeasible. However, the theoretical bounds—which do not suffer from this limitation—demonstrate exponential decay at all tested λ values up to 256, strongly suggesting that the same pattern continues.

5.3 Toward a Full Proof

A complete proof of Conjecture 5.1 requires:

- (1) Formally adapting the compressed oracle technique [11] to Scheme II's specific oracle usage pattern.
- (2) Rigorously applying the Arora et al. lifting framework [1] to show that depth- d quantum oracle interactions reduce to classical transcripts.
- (3) Bounding all error terms in the composition of conjugate coding, conjunction obfuscation, and hash-locking.

Our computational results suggest that all three steps should succeed, with the dominant security loss being the lifting loss of $O(qd/2^{\lambda/4})$.

6 CONCLUSION

We have conducted a systematic computational study of the simulation security of One-Time Memory Scheme II against $\text{BPP}^{\text{QNC}^d}$ adversaries. Through ten experiments spanning adversary depth sweeps, security parameter scaling, oracle query analysis, simulation distance estimation, and component-wise security verification, we provide strong numerical evidence supporting Conjecture 5.1 from [9]. All security metrics decay exponentially in the security parameter λ for polynomial adversary depth d , the conjunction obfuscation achieves perfect indistinguishability for pattern lengths

465 $n \geq 32$, and the sequential POVM bounds confirm the $\cos(\pi/8)^n$
 466 decay rate. The minimum security parameter grows only logarithmically
 467 in adversary parameters, from $\lambda = 104$ at $(d, q) = (4, 16)$
 468 to $\lambda = 144$ at $(d, q) = (256, 256)$, establishing practical parameter
 469 guidance.

470

471 **REFERENCES**

472 [1] Amit Arora, Andrea Coladangelo, Matthew Coudron, Alexandru Gheorghiu,
 473 Uttam Singh, and Hendrik Waldner. 2024. Quantum Depth in the Random Oracle
 474 Model. In *Proceedings of the 56th Annual ACM Symposium on Theory of Computing*
 475 (*STOC*). 1–12.

476 [2] Charles H. Bennett and Gilles Brassard. 2014. Quantum Cryptography: Public
 477 Key Distribution and Coin Tossing. *Theoretical Computer Science* 560 (2014),
 478 7–11. Originally presented at IEEE International Conference on Computers,
 479 Systems and Signal Processing, 1984.

480 [3] Dan Boneh, Özgür Dagdelen, Marc Fischlin, Anja Lehmann, Christian Schaffner,
 481 and Mark Zhandry. 2011. Random Oracles in a Quantum World. *IACR Cryptology*
 482 *ePrint Archive* (2011), 343.

483 [4] Sergey Bravyi, David Gosset, and Robert König. 2018. Quantum Advantage with
 484 Shallow Circuits. *Science* 362, 6412 (2018), 308–311.

485 [5] Anne Broadbent, Gus Gutoski, and Douglas Stebila. 2013. Quantum One-Time
 486 Programs. *IACR Cryptology ePrint Archive* (2013), 13.

487 [6] Nai-Hui Chia, Chi-Ning Chou, Jiayu Zhang, and Ruizhe Zhang. 2022. Classical
 488 Verification of Quantum Depth. *arXiv preprint arXiv:2205.04656* (2022).

489 [7] Matthew Coudron and Shalev Menda. 2020. Computations with Greater Quantum
 490 Depth Are Strictly More Powerful (Relative to an Oracle). *arXiv preprint*
 491 *arXiv:1909.10503* (2020).

492 [8] Shafi Goldwasser, Yael Tauman Kalai, and Guy N. Rothblum. 2008. One-Time
 493 Programs. In *Advances in Cryptology – CRYPTO 2008*. 39–56.

494 [9] Lev Stambler. 2026. Towards Simple and Useful One-Time Programs in the Quantum
 495 Random Oracle Model. *arXiv preprint arXiv:2601.13258* (2026). Conjecture
 496 5.1, Section 5.

497 [10] Stephen Wiesner. 1983. Conjugate Coding. *SIGACT News* 15, 1 (1983), 78–88.

498 [11] Mark Zhandry. 2019. How to Record Quantum Queries, and Applications to
 499 Quantum Indifferentiability. *IACR Cryptology ePrint Archive* (2019), 439.

500 523

501 524

502 525

503 526

504 527

505 528

506 529

507 530

508 531

509 532

510 533

511 534

512 535

513 536

514 537

515 538

516 539

517 540

518 541

519 542

520 543

521 544

522 545

523 546

524 547

525 548

526 549

527 550

528 551

529 552

530 553

531 554

532 555

533 556

534 557

535 558

536 559

537 560

538 561

539 562

540 563

541 564

542 565

543 566

544 567

545 568

546 569

547 570

548 571

549 572

550 573

551 574

552 575

553 576

554 577

555 578

556 579